# DESIGN OF RF CAVITIES FOR THE SPring-8 STORAGE RING

T.Kusaka, T.Yoshiyuki, T.Moro and M.Hara
RIKEN-JAERI Synchrotron Radiation Facility Design Team
2-28-8 Honkomagome, Bunkyo-ku, Tokyo 113 Japan

K.Inoue
Kobe Steel, Ltd.
1-5-5 Takatsukadai, Nishi-ku, Kobe 673-02 Japan

## Abstract

The SPring-8 storage ring has been determined to use 508.6MHz cavities, which are located in four 6.5-m straight sections with low betatron functions. We examined two types of RF systems and compared the RF characteristics of a single-cell cavity and a 3-cell cavity as preliminary studies. The threshold currents due to coupled-bunch instabilities were evaluated based on their measured impedances. Single-cell spherically-shaped cavities were designed to reduce the impedances in higher-order modes and to raise the thresholds above the design current.

## Introduction

An 8GeV synchrotron radiation facility named Spring-8 is now under design [1]. It consists of a storage ring, a booster synchrotron and 1GeV electron and positron linacs. Both the RF systems of the storage ring and the synchrotron operate at a frequency of 508.6MHz, which is identical to the RF frequency of the TRISTAN Main Ring. Since the goal beam current in the storage ring is more than 100mA in a multi-bunch operation, it is necessary to design the RF system in consideration of not only the efficiency of converting RF power into beam power but also beam stability.

## RF system design

The RF parameters of the SPring-8 storage ring are listed in Table 1. The energy loss due to insertion devices is estimated at 3.2MeV based on the typical specifications of insertion devices. The peak RF voltage is 16MV in order to get a sufficiently long quantum lifetime. Four 6.5-m straight sections with low betatron functions are prepared for RF sections and a 1-MW klystron and RF cavities are installed in each section.

Two types of RF systems are advantageous for RF power efficiency, because the input power through an RF window and the dissipated power in a cavity are limited. One system uses thirty-two single-cell cavities and the other uses fourteen 3-cell cavities. Table 2 lists these system parameters. Here, it is assumed that the shunt impedance per unit length is 22.5MΩ/m and the threshold power of a window is 200kW in both systems. Since each cavity has an input coupler, the RF system using single-cell cavities has the ability to accept a higher beam current than the other system. On the other hand, the RF system using 3-cell cavities needs less RF power and includes simpler transmission lines from RF power sources to cavities.

## Preliminary experiments

It is necessary to compare the RF characteristics of two types of cavities. A single-cell cavity with re-entrant nose cones and a 3-cell cavity with inductive coupling slots have been fabricated. The 3-cell cavity is shown in Fig. 1, while the single-cell cavity is assembled with the center cell of the three cells and two end plates. The shunt impedance is optimized by taking the gap size between nose cones as a parameter.

Table 1 RF parameters of the storage ring

| | |
|---|---|
| Beam energy | 8 GeV |
| Beam current (multi-bunch) | 100 mA |
| Circumference | 1429 m |
| Revolution frequency | 210 kHz |
| Radio frequency | 508.6 MHz |
| Harmonic number | 2424 |
| Synchrotron radiation loss in bending magnets | 8.3 MeV |
| Energy loss in Insertion devices | 3.2 MeV |
| Parasitic energy loss per 100 mA | 0.5 MeV |
| Maximum RF voltage | 16 MV |
| Number of 1-MW klystrons | 4 |

Table 2 Comparison between two types of RF systems

| | RF system using single-cell cavities | RF system using 3-cell cavities |
|---|---|---|
| Number of cavities | 32 | 14 |
| Arrangement of cavities | 8 cavities x 4 | 4 cavities x 3<br>2 cavities x 1 |
| Power dissipated in cavities | 1.2 MW | 0.9 MW |
| Total RF power at 100mA | 2.7 MW | 2.3 MW |
| Maximum beam current | 0.2 A | 0.16 A |

The model cavity was machined out of 6061 aluminum alloy. The overall machinery accuracy was within ±0.1mm. Since the coupling slots in the 3-cell cavity were not symmetric to the beam axis, a three-dimensional code MAX3D [2] based on the finite element method was used to investigate the influence of the coupling structure. In the model cavity, two coupling slots whose azimuth was 45 degrees were machined to achieve more than 1% coupling with suppressing the extreme drop of the shunt impedance.

Four modes were precisely measured because they were found to have high impedance values from calculations. Table 3 shows the results of measurement. All impedances are expected for the copper-made cavity and are corrected by using the ratio of the calculated Q-value to the measured Q-value in the fundamental mode. The shunt impedance of the 3-cell cavity was nearly three times as high as that of the single-cell cavity, because a "flat" electric field was achieved in the π mode. The maximum impedance of the 3-cell cavity in the higher-order modes (HOMs) was about 1.5 times as high as that of the single-cell cavity in the TM111-like mode.

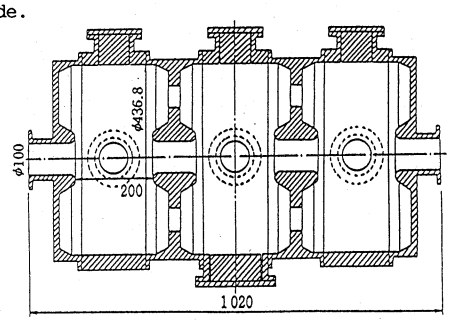


Fig. 1. Cross section of the 3-cell cavity with re-entrant nose cones and coupling slots.

Table 3 Comparison of impedances which are expected values for the copper-made cavity and are corrected by using the ratio of $Q_{calc.}/Q_{exp.}$ for the fundamental mode.

| mode type | Impedance (MΩ or MΩ/m) | |
|---|---|---|
| | Single-cell | 3-cell |
| TM010 | 9.3 | 27 |
| TM011 | 1.8 | 3.4 |
| TM110 | 16 | 24 |
| TM111 | 24 | 35 |

Threshold current due to coupled-bunch instability

The HOMs of accelerating cavities cause a coupled-bunch oscillation in a multi-bunch operation. This oscillation is executed at harmonics of the revolution frequency [3]. Because the spacing between harmonics, 210kHz, is not wide enough compared with the bandwidth of a HOM impedance, it will be difficult to significantly suppress coupled-bunch instabilities by changing the accelerating frequency and the betatron tune in the operation. Therefore, it is necessary to evaluate the threshold beam current of the instabilities, which is approximately calculated by equalizing their growth-rate with the radiation damping rate. The calculated threshold current using the ring parameters and the impedances listed in Table 3 are given in Table 4. Here, only radiation damping due to bending magnets is considered, although contribution by insertion devices is expected. In addition, HOM damping by damping couplers and Landau damping are anticipated. The calculations are carried out on condition that the HOM frequencies of all the cavities are separated so that there is no superposition of the impedance. It will be realizable by adjusting the sizes of blank-flanges of the cavities. Since the transverse impedance of the TM111-like mode is so high, the threshold currents due to transverse coupled bunch instabilities in both RF cavities are lower than 100mA.

Table 4 Threshold beam current due to coupled-bunch instabilities

| type | Threshold current (mA) | |
|---|---|---|
| | Single-cell | 3-cell |
| Longitudinal | 360 | 190 |
| Transverse | 85 | 58 |

## Cavity design

We decided on the following design policies of the cavities for the SPring-8 storage ring after the above studies and the RF system using thirty-two single-cell cavities was chosen.

(1) The intrinsic HOM impedances of the cavities are reduced as much as possible.

(2) The shunt impedance in the accelerating mode is more than 6.8MΩ/cell in order to suppress the excessive thermal load in the cavity.

(3) The cavity structure is made simple in order to ease fabrication, cooling and maintenance.

Since transverse impedances are high in the cavities with re-entrant nose cones, their variation was calculated as a function of the gap length. The results are shown in Fig. 2. It is obvious that the maximum transverse impedance is reduced with the depression of nose cones. Therefore, we made the cavity shape model without nose cones.

The geometry of the cavity in this study is shown in Fig. 3. It consists of two circles connected by a straight line and a flat body. The beam pipe radius was kept at a constant φ100mm. The cavity radius R was adjusted to obtain a 508.6MHz fundamental resonant mode frequency. The cavity length was set to 2*L1=λ/2=294.7mm. The RF characteristics of several

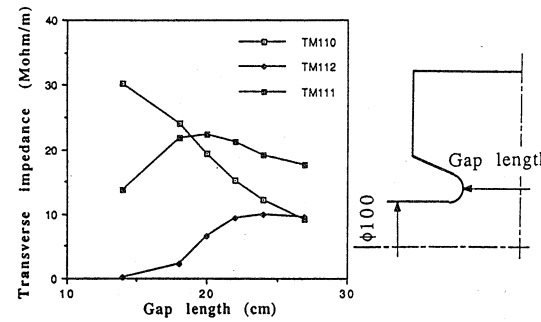


Fig. 2. Variations of transverse impedances as a function of the gap length.

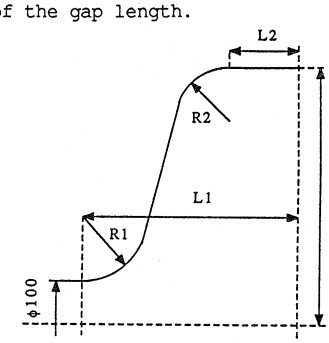


Fig. 3. Cavity shape model with design parameters.

cavities with various combinations of design parameters, R1,R2 and L2, were calculated with the numerical codes SUPERFISH and URMEL. Then, the dependence of the impedances in the four modes on the design parameters were investigated. The results are shown in Fig. 4 (a) through (d). The impedances in TM010-like and TM111-like modes are dependent strongly on a parameter R2+L2. And the impedances in the remaining two modes are relevant to the value of R1. It is necessary to compromise in determining the values of these parameters in order to get the desired shunt impedance in the accelerating mode and reduce the HOM impedances. The variations of other longitudinal impedances were also calculated as a function of cavity

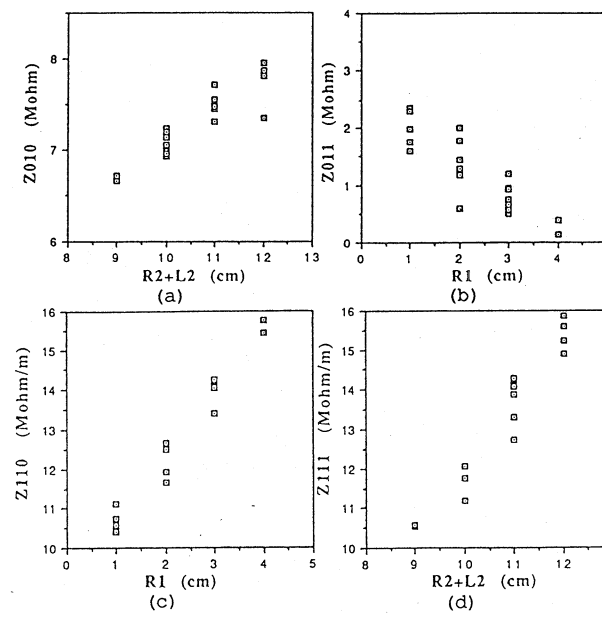


Fig. 4. Dependence of the impedances on the design parameters; (a) in the TM010 mode, (b) in the TM011 mode, (c) in the TM110 mode, (d) in the TM111 mode.

length for cylindrical cavities. The impedances in the TM020-like and TM021-like modes are reduced with the cavity length.

Four design parameters, R1, R2, L1 and L2, were adjusted to reduce all HOM impedances. In this process, priority was given to the impedances in lower resonant frequencies, because HOM frequencies in the thirty-two different cavities are easily separated in higher frequencies. The designed RF cavity is shown in Fig. 5. It is a spherically-shaped cavity similar to the superconducting cavities now widely used. The computed impedances are shown in Fig. 6, compared with the ones of the re-entrant model cavity. The shunt impedance in the accelerating mode is 7.4MΩ, which is about 20% lower than the one of the re-entrant cavity. However, the maximum transverse impedance decreases by approximately one-half. Therefore, coupled-bunch instabilities are suppressed and the threshold current is raised above 100mA.

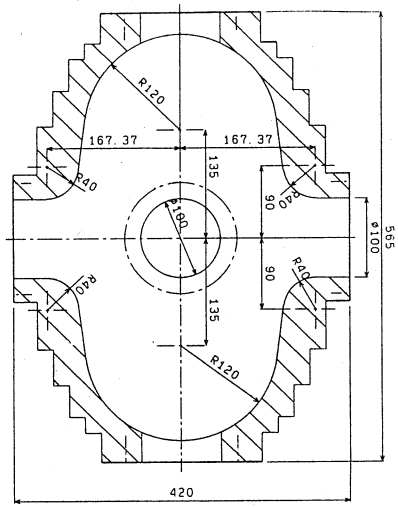


Fig. 5. Cross section of the designed spherically-shaped cavity.

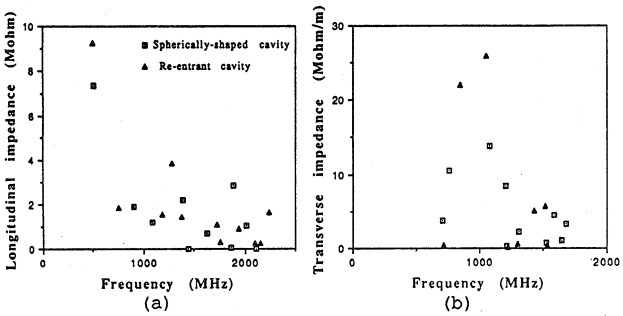


Fig. 6. Comparison of computed impedances between two types of cavities; (a) in longitudinal impedances, (b) in transverse impedances.

## Thermal analysis of the cavity

It is important to calculate the temperature distribution and dimensional changes in the cavity structure and to estimate the loss in shunt impedance resulting from the decrease of electrical conductivity. In the RF system of the SPring-8 storage ring, 40kW of RF power will be dissipated in the wall of the single-cell cavity. The power is distributed as shown in Fig. 7.

A general purpose computer code, ABAQUS [4], based on the finite element method was used to calculate the thermal characteristics of the cavity. The cavity is

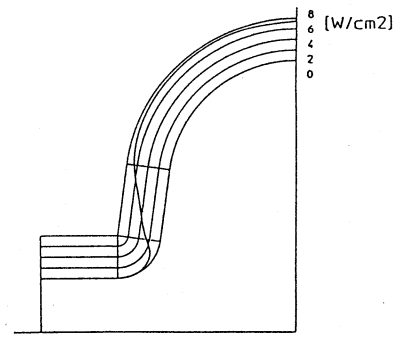


Fig. 7. Power distribution at a total power of 40kW/cell.

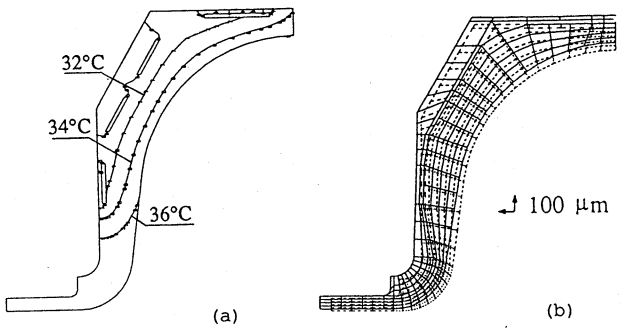


Fig. 8. (a) Temperature distribution of the cavity; (b) deformation of the cavity; the dashed lines show the original mesh and the solid lines show the displaced mesh.

cooled by eight parallel thin channels along the cavity wall. The temperature distribution is shown in Fig. 8 (a), when the velocity of the cooling water is 1.5m/s and the initial temperature of the cavity is 20°C. The increase of the surface temperature is about 16°C uniformly. Therefore, the loss in shunt impedance is estimated to be less than 4%. Figure 8 (b) shows deformation due to thermal stress. The resonant frequency change is calculated to be about 80kHz and it can be easily compensated with a frequency tuner.

## Conclusion

The RF system using thirty-two single-cell cavities is adopted for the SPring-8 storage ring. The cavities were designed to be spherically-shaped in order to reduce the HOM impedances. We are going to fabricate a model cavity and confirm the RF characteristics. Furthermore, high power tests using a 1-MW klystron are planned to determine the detailed specification of the practical cavities.

## References

[1] M.Hara et al., "Storage Ring Design for the 8 GeV Synchrotron Radiation Facility in Japan," 14th International Conference on High Energy Accelerator, August, 1989, Tsukuba, Japan.

[2] M.Hara et al., "Three Dimensional Analysis of RF Electromagnetic Field by the Finite Element Method," Proc.11th Int. Conf. on Cyclotrons and their Applications, pp.337-340, 1987.

[3] H.Kobayakawa et al., "Critical Test of Coupled-Bunch Instability Theory," Jpn. J. Appl. Phys., 25, pp.864-874, 1986.

[4] Hibbitt, Karlsson & Sorensen, Inc., "ABAQUS User's Manual," 1988.